

RSC Advances



This is an *Accepted Manuscript*, which has been through the Royal Society of Chemistry peer review process and has been accepted for publication.

Accepted Manuscripts are published online shortly after acceptance, before technical editing, formatting and proof reading. Using this free service, authors can make their results available to the community, in citable form, before we publish the edited article. This *Accepted Manuscript* will be replaced by the edited, formatted and paginated article as soon as this is available.

You can find more information about *Accepted Manuscripts* in the [Information for Authors](#).

Please note that technical editing may introduce minor changes to the text and/or graphics, which may alter content. The journal's standard [Terms & Conditions](#) and the [Ethical guidelines](#) still apply. In no event shall the Royal Society of Chemistry be held responsible for any errors or omissions in this *Accepted Manuscript* or any consequences arising from the use of any information it contains.

Role of ionic liquid [BMIMPF₆] in modifying the crystallization kinetics behavior of polymer electrolyte PEO-LiClO₄

S.K. Chaurasia^{a,b}, Shalu^a, A.K. Gupta^a, Y.L. Verma^a, V.K. Singh^a, A.K. Tripathi^a, A. L. Saroj^a
and R. K. Singh^{a,*}

^a Department of Physics, Banaras Hindu University, Varanasi-221005, India

^b Department of Physics and Astrophysics, University of Delhi, Delhi-110007, India

Abstract

We report on the modification in crystallization kinetics behavior of PEO+10wt.% LiClO₄ polymer electrolyte by the addition of ionic liquid, 1-ethyl-3-methylimidazolium hexafluorophosphate (BMIMPF₆). Three techniques have been used for studying crystallization kinetics viz. (i) isothermal crystallization technique using DSC (ii) nonisothermal crystallization technique using DSC (iii) and by monitoring the growth of spherulites with time in the polymer electrolyte films using polarizing optical microscope (POM). Results from all the three techniques show that the presence of ionic liquid BMIMPF₆ suppresses the crystallization rate due to its plasticization effect. Isothermal crystallization data was well described by the Avrami equation and Avrami exponent n lies in the range of 1 to 2, which signifies 2D crystal growth geometry occurring in these polymer electrolytes under investigated temperature range. However, Avrami crystallization rate constant 'K' increases exponentially with crystallization temperature as well as ionic liquid content. However, the non-isothermal crystallization kinetics of these polymer electrolytes is discussed in terms of three different models (Jeziorny's, Ozawa's and Li and coworkers) and it is found that Li and Mo's method better explains the non-isothermal crystallization data. In addition, crystalline morphology and spherulite growth were studied by POM, which shows the suppression in crystallization in the presence of ionic liquid as confirmed by spherulite growth rate (G_s) analysis.

Keywords: Polymer electrolyte, Ionic liquids, Crystallization kinetics, Spherulite growth,

Corresponding author: Tel: +91 542 2307308; Fax: +91 542 2368390

Email address: * rksingh_17@rediffmail.com

Introduction

Development of ion conducting materials (like polymers, gels, glasses etc.) recently attracted a global interest for developing a variety of electrochemical devices like rechargeable batteries, fuel cells, supercapacitors, solar cells, actuators, etc.¹⁻⁵ A straight forward strategy adopted for this is to integrate mobile ionic species into different solid/polymeric soft matrices. Polymers have advantage over other ion conducting materials because it exhibits various favorable properties such as ease of fabrication in thin film form and is mechanically, thermally and electrochemically more stable.⁶ One of the necessary conditions, apart from thermal/mechanical/chemical stability, is to make polymer backbone conducive for providing high ionic mobility for the movement of ions. Earlier, many ion conducting polymer matrices or polymer electrolytes were formed by complexing ionic salts (like Li^+ , Na^+ , Mg^{2+} , Zn^{2+} etc.) with polar polymers (like PEO, PMMA, PVA, PVdF) and were much studied but their room temperature ionic conductivity is very low ($\sim 10^{-6}$ - 10^{-7} S cm^{-1}) because of its high degree of crystallinity which hinders the motion of the ions in the polymer network.⁷⁻¹¹ Therefore, various approaches have been adopted to improve their ionic conductivity which includes (a) addition of low molecular weight plasticizers/organic carbonates¹²⁻¹³ like ethylene carbonate (EC), propylene carbonate (PC), diethyl carbonate (DEC) and (b) use of inorganic fillers¹⁴⁻¹⁶ like SiO_2 , Al_2O_3 , CNT, TiO_2 . Use of conventional plasticizers in polymer electrolytes can enhance the ionic conductivity by lowering their glass transition temperature (T_g) which further increases the amorphous phase of the polymer matrix and also causes poor mechanical and thermal stability and have narrower electrochemical potential window due to their volatile nature that limits their application in devices.¹⁷ Recently, a new approach has been adopted to enhance the ionic conductivity of the polymer electrolyte membranes by incorporating ionic liquids (ILs) in the

polymer matrix.¹⁸⁻²⁰ ILs have attracted much attention as an excellent alternative to the conventional plasticizers due to their distinct properties such as wide liquidus range, non-volatility, non-flammability, negligible vapour pressure at room temperature, wide electrochemical stability window, high ionic conductivity and excellent thermal and chemical stability.²¹⁻²³ ILs are entirely composed of bulky and asymmetric organic cations and inorganic anions. Due to unique properties of ILs, polymer electrolytes based on ionic liquid offer high conductivity along with improved thermal and mechanical properties. In polymer electrolytes, ionic liquid plays the role of a plasticizer as well as a supplier of free charge carriers for the ion conduction.²⁴

In most of the polymer electrolytes, the amorphous phase is found to be more conducting than crystalline phase. Accordingly, it is very important to learn about the crystallization kinetics behavior of polymer as well as polymer electrolytes.²⁵⁻²⁸ Crystallization is a process of phase transformation that involves transformation of disordered amorphous phase into single or multi ordered phase. Polymer crystallization is a complex process which affects the final properties of the materials.²⁹ It is also observed that some polymers can crystallize while some cannot. Among the ones that can, the degree of crystallization, the structure of crystal and their size depend upon a number of parameters, such as temperature, time, and concentration of solution, stress present during the crystallization.³⁰ Some studies are available in literature on the modification in crystallization behaviour of polymers on the addition of complexing salts³¹ or by changing its molecular weight³², using inorganic fillers³³, carbon nanotubes³⁴, and also in confined geometries.³⁵ Polymer PEO is known to be a “*semicrystalline*” polymer which consist of both crystalline and amorphous phases and its high capability in forming complexes with many salts as well as its high chemical stability led to emerge as a promising host matrix for the preparation

of polymer electrolytes. However, PEO tends to crystallize due to its highly ordered chain structure, which impedes the ion transport in the polymeric matrix. This is a general observation for semicrystalline polymer electrolytes and well documented in literature.³⁶⁻³⁷ Therefore, it would be interesting to study the crystallization kinetics behavior of such a semicrystalline polymer PEO including crystal structure, crystalline morphology etc. Degree of crystallinity is of particular interest for the better understanding of the structure property relation to significantly improve the performances of the solid state devices containing PEO based polymer electrolytes.

This paper reports the crystallization kinetics behavior of polymer electrolyte (PEO+10 wt.% LiClO₄) with different amounts of added ionic liquid (BMIMPF₆). Crystallization kinetics has been studied by isothermal and non-isothermal crystallization method using DSC and affirmative confirmation of the crystallization behavior is obtained by examining the expansion of spherulites by polarizing optical microscope (POM). It has been found that the addition of BMIMPF₆ in (PEO+10 wt.% LiClO₄) slows down the crystallization rate due to plasticization effect of ionic liquid, BMIMPF₆.

Experimental Section

Materials and method

The starting materials used for the preparation of polymer electrolyte films are poly (ethylene oxide), PEO of average mol. wt. 6×10^5 g mol⁻¹, lithium salt LiClO₄ and ionic liquid, (1-butyl-3-methylimidazolium hexafluorophosphate, BMIMPF₆) obtained from Sigma Aldrich. The ionic liquid, BMIMPF₆ was vacuum dried at 10⁻⁶ torr for 24 hrs before use.

Polymer electrolyte films of PEO+10wt.% LiClO₄+ xwt.%BMIMPF₆ for x=0, 5, 10, 15 and 20 were prepared by solution casting method. The particular weight ratio of 10 wt.% LiClO₄ in PEO was chosen for incorporating varying amounts of ionic liquid BMIMPF₆ to prepare PEO+10wt.% LiClO₄+xwt.%BMIMPF₆ polymer electrolyte films because of its excellent mechanical stability as well as reasonable ionic conductivity compared to other high lithium salt containing samples. Though, the high conducting films containing higher loading of lithium salt LiClO₄ could be prepared without BMIMPF₆ but on loading of ionic liquid BMIMPF₆ these films tend to become unstable. In solution casting method, polymer PEO was dissolved in methanol under stirring at 40 °C and then requisite amount of LiClO₄ was added and stirred until it appears in the form of homogeneous solution. After that, required amount of BMIMPF₆ was added in the above solution and stirred again for 2-4 hrs until a viscous solution was obtained. The viscous solution so obtained was poured into polypropylene petridishes. After complete evaporation of the solvent, PEO+10wt.% LiClO₄+xwt.%BMIMPF₆ polymer electrolyte films containing different amounts of BMIMPF₆ were obtained. These films were vacuum dried before further use.

Three methods viz. isothermal, non-isothermal and optical microscopic study have been used for studying the crystallization kinetics. The isothermal and non-isothermal crystallization kinetics of the prepared samples were performed using a differential scanning calorimeter (Mettler Toledo DSC1 system). All the DSC measurements were conducted under a nitrogen atmosphere. The detailed procedure of isothermal and non-isothermal method are given in their respective sections where results are discussed.

For studying the crystalline morphology and spherulite growth rate, Lietz DMR polarizing microscope was used. All the polarizing optical microscopy (POM) studies were done at a magnification of 50X. For carrying out the POM-studies, the samples were first heated above melting temperature (T_m) of polymer electrolyte films and held there for some time till a complete isotropic amorphous phase was observed in POM. Then, the polymer films were quickly quenched to the desired temperature of crystallization (these temperature are less than T_m of the polymer electrolytes). The size of spherulites as a function of time elapsed after initial appearance of the spherulites was monitored by POM for crystallization study.

Crystallization kinetics by isothermal method

For carrying out the actual experiment, the samples were heated up to ~ 75 °C (above the melting temperature of polymer T_m) and held there for 5 min to erase the thermal history and then, quickly cooled to the temperature at which crystallization is desired to be studied (note that these temperatures are less than $(T_m)_{onset}$ as determined by DSC thermograms). The samples were maintained at desired crystallization temperature, viz. $T_c = 44, 46, 48$ and 50 °C to crystallize and DSC exothermic curves for heat flow vs. time were recorded. These DSC isothermal curves obtained for different samples were used for studying the crystallization kinetics by isothermal method. The heat flow vs. time plot for (PEO+10 wt.% LiClO₄)+x wt.%BMIMPF₆ films for x=0, 10 and 20 are shown in Fig. 1. It can be seen that with increasing the crystallization temperature, the crystallization exothermic peak becomes flatter possibly due to increase in the flexibility of polymer PEO backbone which suggest that samples relatively take longer time to crystallize as we approach to the $(T_m)_{onset}$ of the samples.

The crystallization kinetics of polymers under isothermal condition is described by the well known Avrami equation³⁸ in terms of the dependence of relative crystallinity (X_t) on the crystallization time (t) as follows:

$$X_t = 1 - \exp(-Kt^n) \quad (1)$$

where X_t is the relative crystallinity generated at any time t, n is the Avrami exponent and depends on the nucleation and growth geometry of the crystal, and K is the overall crystallization rate constant associated with nucleation as well as growth contributions.

The relative crystallinity (X_t) generated at any time (t) can be obtained by using the DSC exothermic isothermal curves as illustrated in Fig. 1. The relative crystallinity (X_t), is defined as the ratio of crystallinity generated at any time t to the crystallinity when time approaches to infinity. X_t has been evaluated using the following relation:

$$X_t = \frac{\Delta H_t}{\Delta H_\infty} = \frac{\int_0^t \left(\frac{dH}{dt} \right) .dt}{\int_0^\infty \left(\frac{dH}{dt} \right) .dt} \quad (2)$$

where dH/dt is the rate of heat evolution, ΔH_t is the total heat evolved at any time t and ΔH_∞ is the heat evolved when time approaches to infinity (∞).

Obviously, the values of X_t at a given crystallization time t can be obtained by integrating the area of exothermic DSC isothermal curves between time t = 0 to t divided by the whole area of the exothermic peaks.

Using eqn. 2, the conversion curves of X_t (the crystallized fraction) versus t for (PEO+10 wt.% LiClO₄)+x wt.%BMIMPF₆ films for x = 0, 5 and 10 at various crystallization temperatures

($T_c = 44, 46, 48$ and $50\text{ }^\circ\text{C}$) are shown in Fig. 2. All the curves show sigmoid characteristics with time and shift towards higher time regime as the crystallization temperature (T_c) increases. These features indicate that, at higher T_c , the crystallization rates become slow and samples take more time to crystallize because we are approaching near $(T_m)_{onset}$. Further, a comparison of results of polymer electrolyte PEO+10 wt.% LiClO₄ (see Fig. 2, curve 'a') with those polymer electrolyte films doped with ionic liquid, BMIMPF₆ (see Fig. 2, curves b and c) showed that BMIMPF₆ containing samples take longer time to crystallize in comparison to pristine polymer electrolyte due to the increase in amorphicity of the samples.³⁹ For example, we can see that the pristine polymer electrolyte PEO+10 wt.% LiClO₄ took nearly 1.8 min to obtain complete crystallization at $T_c = 44\text{ }^\circ\text{C}$ and time required to finish crystallization for 5 wt.% BMIMPF₆ containing polymer electrolyte slightly increases and found to be ~ 2 min at the same crystallization temperature, while at higher T_c (say $50\text{ }^\circ\text{C}$), it takes ~ 15 min to complete crystallization (for detail see Fig. 2c).

These observations clearly indicate that with increasing the crystallization temperature or ionic liquid concentration, the samples take longer time to crystallize because of the plasticization effect of ionic liquid.⁴⁰⁻⁴² In our previous studies⁴³⁻⁴⁴ on the crystallization kinetics of polymer PEO upon inclusion of ionic liquid as well as lithium salt it has been shown that the crystallization rate of PEO changes more on addition of BMIMPF₆ alone rather than for (PEO+LiClO₄) because the plasticization effect of ionic liquid is less felt by the latter which has already been amorphosized by the addition of LiClO₄. This effect will become more clear later when we discuss the results of crystallization half time ($t_{1/2}$) given in the next section.

The crystallization half time ($t_{1/2}$), which is defined as the time necessary to attain 50 % of the final crystallinity of the samples, is an important parameter for discussing the

crystallization kinetics.⁴⁵ The values of $t_{1/2}$ are directly obtained from Fig. 2, from which rate of crystallization ($G=1/t_{1/2}$) can be calculated. Greater is the value of $t_{1/2}$, lower is the rate of crystallization. Fig. 3 shows the variation of G for (PEO+10wt.% LiClO₄)+x wt.% BMIMPF₆ at various crystallization temperatures (T_c). As illustrated in Fig. 3, the values of G decrease with increasing T_c for all the samples, indicating that the overall crystallization rate becomes slow at higher T_c because the nucleation process is more difficult at higher crystallization temperatures.⁴⁶ Further, it may be remarked here that the values of G ($=1/t_{1/2}$) obtained for (PEO+10 wt.%LiClO₄)+x wt.% BMIMPF₆ films are lower in comparison to that of pristine polymer electrolyte PEO+10 wt.%LiClO₄ at a given T_c as shown in Fig. 3, which clearly indicates the slow down of the crystallization rate by the incorporation of BMIMPF₆. In addition, the reduction in overall crystallization rate, G of polymer electrolytes with increasing BMIMPF₆ concentration is attributed to the fact that the presence of ionic liquid, BMIMPF₆ exerts a dilution effect for the crystallizable polymer PEO due to the plasticization effect of ionic liquid. Our previous studies⁴⁷⁻⁴⁹ also showed such type of situation in which the effects of ionic liquid on the properties of polymers and polymer electrolytes were studied and it was revealed that the ionic liquid acts as an efficient plasticizer.

Avrami plots (i.e. double logarithmic graphic representation of crystallization data) are generally used to calculate the values of n and K . It can be obtained by taking the double logarithmic of eqn. 1 and written as:

$$\log[-\ln(1 - X_t)] = \log K + n \log t \quad (3)$$

According to eqn 3, the plot of $\log [-\ln(1-X_t)]$ vs. $\log t$ should be a straight line. In the present study, the Avrami plots for PEO+10 wt.% LiClO₄ films containing different amounts of BMIMPF₆ give rise to a series of parallel straight lines at different crystallization temperatures (viz. $T_c = 44, 46, 48$ and 50 °C) as shown in Fig. 4. After linear fitting of these plots by a straight line at different T_c , both Avrami exponent 'n' and crystallization rate constant 'K' can be obtained by knowing the slope and intercept of the straight line, respectively. The various Avrami parameters obtained from isothermal crystallization method for PEO+10 wt.% LiClO₄+x wt.%BMIMPF₆ at various crystallization temperatures are given in Table 1.

It is known that the values of Avrami exponent are the consequences of geometry of specific crystal dimension and have been used to specify the dimension of growing crystals. The value of Avrami exponent n is assumed to lie in the range between 1 to 4 and related to the geometry characteristics of the growing crystals: n =1 is ascribed to the 1D structure, 2 is ascribed to the 2D structure, and 3 or 4 ascribed to the 3D structure.⁵⁰ In the present study, the values of 'n' for all the polymer electrolyte (PEO+10 wt.% LiClO₄)+x wt.% BMIMPF₆ films lie between 1 and 2 at all studied crystallization temperatures. This indicates that the 2D crystal growth morphology dominates at all temperatures at which crystallization was studied.

The effect of incorporation of ionic liquid into the polymer membrane, apart from decreasing the rate of crystallization is also expected to reflect itself the values of activation energy for crystallization. To check this, we determined this activation energy for PEO+10wt.% LiClO₄ polymer electrolyte with BMIMPF₆. The Avrami crystallization rate constant K can be assumed to be a consequence of a thermally activated process and has been used to determine the

activation energy for crystallization.⁵¹ The crystallization rate constant, K can be expressed by the Arrhenius equation as follows:

$$K^{1/n} = K_o \exp(-\Delta E / RT_c) \quad (4)$$

Equation 4 can also be written as:

$$\ln K^{1/n} = \ln K_o - \Delta E / RT_c \quad (5)$$

where K_o is the pre-exponential factor independent of temperature, ΔE is the isothermal crystallization activation energy, R is the gas constant and T_c is the crystallization temperature.

By plotting the $\ln K^{1/n}$ versus $1/T_c$, ΔE can be obtained by the slope of these curves. Typical plot for PEO+10 wt.% LiClO₄+10wt.% BMIMPF₆ are shown in Fig. 5. The slope of this curve gives the value of $\Delta E/R$, from which the isothermal crystallization activation energy ΔE can be directly calculated. The value of isothermal crystallization activation energy, ΔE for (PEO+10 wt.% LiClO₄)+10wt.% BMIMPF₆ polymer electrolyte was found to be 97 KJ/mol.

Crystallization kinetics by non-isothermal method

Non-isothermal crystallization method using DSC is also one of the most convenient methods for studying the crystallization kinetic behavior of polymers. In this method, samples were heated above the melting temperature of the polymer PEO (~70 °C), kept there for 5 min to erase the thermal history and then cooled at different cooling rates (viz. 5, 10, 15 and 20 °C/min). DSC exothermic curves for heat flow versus temperature were recorded to analyze the non-isothermal crystallization data. Samples used for non-isothermal crystallization were the same

for which isothermal crystallization kinetic studies were carried out. The DSC exothermal curves for (PEO+10 wt.% LiClO₄)+x wt.% BMIMPF₆ films at different cooling rates 5, 10, 15 and 20 °C/min are shown in Fig. 6. It can be seen that the exothermic crystallization peaks were shifted to lower temperature side and became broader with increasing cooling rates. In order to know the non-isothermal crystallization kinetics, relative crystallinity (X_t) versus temperature plots for these polymer electrolyte films were obtained using eqn. 2 and are shown in Fig. 7 (procedure is similar to that used for isothermal crystallization method described earlier). Fig. 7 shows the plots of X_t versus temperature (T), which illustrate an anti-S shaped characteristic. In the non-isothermal crystallization process, temperature scale of X_t versus T plots could be converted into X_t versus t using the following relation:⁵²

$$t = \frac{T_o - T}{\phi} \quad (6)$$

where t is the crystallization time, T_o is the onset temperature of crystallization ($t=0$), T is the crystallization temperature and ϕ is the cooling rate. Using eqn. (6), the plot of relative crystallinity versus temperature (X_t vs. T) can be easily transformed to the plot of relative crystallinity versus time (X_t vs. t). The X_t vs. t plots for (PEO+10 wt.% LiClO₄)+x wt.%BMIMPF₆ films for x=0,5,10,15 and 20 are given in Fig. 8. It showed that higher the cooling rate, shorter the time to complete crystallization and vice versa.

Several approaches have been used for describing the crystallization process involved in the non-isothermal crystallization kinetics, which are based on various models including modified Avrami equation by Jeziorny⁵³, Ozawa analysis⁵⁴ and Liu and Mo method⁵⁵. These approaches are discussed below:

Modified Avrami equation: The modified Avrami⁵³ equation is frequently used to analyze the non-isothermal crystallization process. Considering the non-isothermal crystallization character of the process, Avrami equation can be written as:

$$X_t = 1 - \exp(-Z_t t^{n'}) \quad (7)$$

where n' is a constant depending on the type of nucleation and crystal growth dimension known as non-isothermal Avrami exponent, and Z_t is the non-isothermal crystallization rate constant and depends on nucleation and growth parameters. The values of n' and Z_t were obtained from the slope and intercept of straight regime of plots drawn between $\log[-\ln(1 - X_t)]$ and $\log t$. The $\log[-\ln(1 - X_t)]$ vs. $\log t$ plots for (PEO+10 wt.% LiClO₄)+x wt.%BMIMPF₆ for x=0,5,10,15 and 20 at different cooling rates (viz. 5, 10, 15 and 20 °C/min) are shown in Fig. 9. From these plots, we can see that at initial stages, these curves are fitted well by eqn. (7) but deviate from the linear relation on higher crystallization. Therefore, we can say that the Avrami equation cannot be accurately used for describing the entire non-isothermal crystallization kinetics process.

Jeziorny⁵³ modified the Avrami equation for non-isothermal crystallization process, it assumes that curves with a fixed cooling rate represent a series of isothermal crystallization process and gave a modified non-isothermal crystallization rate (Z_c) in which the effect of cooling rate ' ϕ ' on the value of Z_t was included as under:

$$\log Z_c = \frac{\log Z_t}{\phi} \quad (8)$$

The values of Avrami constants n' and Z_c obtained by modified Avrami equation in non-isothermal crystallization method are given in Table 2. It may be remarked here that the values

of n' and Z_c obtained in non-isothermal crystallization do not have the same magnitude as in the isothermal method due to different experimental conditions used in these two methods.

Ozawa Analysis: Ozawa⁵⁴ extended the Avrami equation by considering that the non-isothermal crystallization process consists of a large number of infinitesimal isothermal crystallization steps. According to Ozawa theory, the non-isothermal crystallization process can be described by the following equation as:

$$X'_T = 1 - \exp\left(-\frac{K^*(T)}{\phi^m}\right) \quad (9)$$

where X'_T is the relative crystallinity at temperature T , ϕ is the cooling rate, m is the Ozawa exponent, $K^*(T)$ is the cooling function related to the overall crystallization rate, m is the Ozawa exponent which depends on the dimension of the crystal growth. The above equation (9) can also be expressed as

$$\log\left[-\ln(1 - X'_T)\right] = \log K^*(T) - m \log \phi \quad (10)$$

If Ozawa theory is fully applicable in describing the non-isothermal crystallization process then the plot of $\log\left[-\ln(1 - X'_T)\right]$ vs. $\log \phi$ should be a straight line which was not the case for our samples as shown in Fig. 10. So, Ozawa equation cannot be fully applicable for describing the non-isothermal crystallization process of PEO+10 wt.% LiClO₄ polymer electrolytes as well as PEO+10 wt.% LiClO₄+xwt.% BMIMPF₆ containing different amounts of BMIMPF₆.

Li and Mo's Method: The kinetic equation proposed by Liu and coworkers⁵⁵ based on the combination of Ozawa and Avrami equations was frequently used for describing the non-isothermal crystallization process. This method has been successfully applicable for describing the non-isothermal crystallization behavior of many polymeric systems.⁵⁶⁻⁵⁷ The general form of this equation can be written as:

$$\log \phi = \log F(T) - b \log t \quad (11)$$

where $\log F(T) = [K^*(T)/Z_t]^{1/m}$ and b is the ratio between the Avrami and Ozawa exponents n and m. Here, the function F(T) refers to the value of cooling rate required to reach a defined degree of crystallinity at a certain temperature in unit crystallization time.⁵⁸ The higher value of F(T) gives lower crystallization rate. The plot between $\log \phi$ and $\log t$ for (PEO+10 wt.% LiClO₄)+x wt.%BMIMPF₆ films at different cooling rates and various crystallinity gives a straight line as shown in Fig. 11. From the intercept and slope of which respectively the values of $\log F(T)$ and b can be obtained for the samples for different values of 'x'. These values are listed in Table 3. From this, we can see that for a given degree of crystallinity (say 10 %), the value of $\log F(T)$ for PEO+10 wt.% LiClO₄ polymer electrolyte is 0.607 which become to 0.629, 0.634, 0.688 and 0.714 respectively for polymer electrolyte containing 5, 10, 15 and 20 wt.% BMIMPF₆. In general, the value of F(T) for all the polymeric films is found to increase with increasing amount of BMIMPF₆ in PEO+10 wt.% LiClO₄. The above feature clearly indicates that the incorporation of ionic liquid into PEO+10 wt.%LiClO₄ polymer electrolyte decreases the crystallization rate due to the plasticization effect of an ionic liquid.⁵⁹⁻⁶¹ The presence of ionic

liquid BMIMPF₆ into PEO+LiClO₄ polymer electrolyte hinders the crystallization of polymer and leads to slow down the crystal growth rate as confirmed by the morphological studies.

Kissinger Analysis: It has been already shown by isothermal crystallization kinetics study that the incorporation of BMIMPF₆ in PEO+10 wt.%LiClO₄ polymer electrolyte changes the activation energy of the crystallization. We have re-confirmed this assertion from non-isothermal kinetic study also. The crystallization activation energy for non-isothermal crystallization process can be obtained by the Kissinger method.⁶² In this method, the effect of various cooling rates (ϕ) on the crystallization peak temperature (T_p) has been studied. The crystallization activation energy ($\Delta E'$) for non-isothermal process using Kissinger method can be expressed as:

$$\frac{d[\ln(\phi/T_p^2)]}{d(1/T_p)} = \frac{-\Delta E'}{R} \quad (12)$$

where R is the gas constant and ϕ is the cooling rate. The slope of the plot $\ln(\phi/T_p^2)$ vs. $1/T_p$ gives a straight line, from which by knowing the value of $\Delta E'/R$, $\Delta E'$ can directly be calculated. Typical Kissinger plot for (PEO+10wt.%LiClO₄)+10wt.%BMIMPF₆ polymer electrolyte are shown in Fig. 12. The value of $\Delta E'$ obtained for (PEO+10wt.%LiClO₄)+10wt.% BMIMPF₆ polymer electrolyte was found to be 37 KJ/mol. This value is somewhat lower than those obtained for isothermal crystallization method earlier because of the different experimental conditions in the two methods. In non-isothermal crystallization method, temperature changes constantly which affects the rate of nuclei formation as well as spherulie growth.

Crystalline morphology and spherulite growth by polarized optical microscopy

When polymers are crystallized from the melt, the most common of the observed structures are the spherulites. These spherulites are in the form of spherical aggregates of lamellae, characteristics of polymers crystallized isothermally in the absence of pronounced stress or flow.⁶³⁻⁶⁵ Typical dimensions of spherulites are of the order of microns and sometimes, even millimeters. Therefore, they can be easily viewed under a polarizing optical microscope. The spherulites continue to grow radially until they impinge upon one another. A measure of their growth until the time of impingement provides a wealth of information regarding the mechanism of crystallization in the polymer, and has been the focus of several investigations.⁶⁶⁻⁶⁸

The number and size of spherulites growing in the polymer matrix controls the overall crystallinity of the polymer. Therefore, measuring the size of spherulites as a function of time can give an idea about the rate of crystallization. This technique has been used by us for measuring the rate of crystallization of our polymer electrolyte membranes. The size of spherulite has been measured by polarized optical microscope (POM). Typical growth of such spherulites appearing in PEO+10 wt.% LiClO₄ and (PEO+10wt.% LiClO₄)+10 wt.% BMIMPF₆ polymer electrolyte films at different time and crystallized at 50°C are shown in Fig. 13. We can see that spherulite growth was very fast for PEO+10wt.% LiClO₄ polymer electrolyte and within 10 seconds it acquired ~100 μm diameter and then its size increased to 310 μm when elapsed time was 120 sec as shown in Fig. 13 curve 'a (i) and (v)'. As BMIMPF₆ was added in PEO+10wt.% LiClO₄ polymer electrolyte, then spherulite size was reduced and number of nucleating sites increased. This is evident when we compare Fig. 13 curves a(i-v) with b (i-v).

In the present case, we can also see that the size of one particular spherulite at any particular snap increased with time as indicated in rectangle in Fig. 14 a(i-iv) and b(i-iv). Therefore, it is important to find out the spherulitic Growth rate (and hence crystallization rate) and for deciding the effect of BMIMPF₆ on the crystallization behavior of polymer electrolytes with and without ionic liquid. The spherulite size vs. time plot for PEO+10wt.% LiClO₄ polymer electrolyte and with added 10 wt.% BMIMPF₆ is shown in Fig. 14, whose slope gives the spherulites growth rate (G_s). The value of G_s for pure PEO+10wt.% LiClO₄ is found to be 1.77 $\mu\text{m}/\text{sec}$ which decreased to 0.67 $\mu\text{m}/\text{sec}$ for (PEO+10wt.% LiClO₄)+10 wt.% BMIMPF₆. The above observation clearly indicates that the incorporation of BMIMPF₆ in PEO+10wt.% LiClO₄ polymer electrolyte hinders the spherulites growth rate of polymer PEO. This supports our previous results obtained from isothermal and non-isothermal DSC technique that indicate the suppression in the crystallization rate of polymer PEO due to the incorporation of an ionic liquid (BMIMPF₆) owing to its plasticization effect as discussed earlier in this paper.

Conclusions

The crystallization kinetics behavior of (PEO+10 wt.% LiClO₄)+x wt.% BMIMPF₆ polymer electrolytes has been studied by using three techniques viz. isothermal and non-isothermal crystallization method using DSC as well as monitoring spherulitic growth using polarizing optical microscope. The well known Avrami equation has been used to describe the isothermal crystallization process. The obtained crystallization parameters for isothermal crystallization such as Avrami exponent (n), crystallization rate constant (K), crystallization half time ($t_{1/2}$), crystallization rate (G) and isothermal crystallization activation energy (ΔE) suggested that the incorporation of the ionic liquid, BMIMPF₆ into PEO+10wt.% LiClO₄ polymer electrolyte

hinders the crystallization of polymer PEO due to the plasticization effect. The value of Avrami exponent 'n' obtained for isothermal crystallization process of PEO+10wt.% LiClO₄+x wt.% BMIMPF₆ for x=0, 5 and 10 was found to be less than 2, indicating the 2D crystal growth geometry. It was also found that the non-isothermal crystallization data cannot be fully described by the modified Avrami equation (Jeziorny method) and Ozawa analysis. It has observed that the method proposed by Li and coworkers was employed to analyze the non-isothermal crystallization process accurately. POM study shows that the incorporation of BMIMPF₆ in PEO+10wt.% LiClO₄ polymer electrolyte slows down the spherulite growth rate as observed by spherulite size vs. time plots. All the three techniques used by us to study the effect of ionic liquid BMIMPF₆ on crystallization behavior of polymer electrolyte have led to the conclusion that the presence of BMIMPF₆ suppresses the crystallization rate. This will have an effect in decreasing the absolute crystallinity of PEO with increasing BMIMPF₆ content.

Acknowledgements

One of us (RKS) is grateful to BRNS-DAE Mumbai and DST New Delhi, India for financial assistance for carrying out this work and SKC is thankful to UGC New Delhi, India for providing the Dr. D. S. Kothari Postdoctoral research fellowship.

References

1. J. R. MacCallum, C. A. Vincent, Polymer Electrolyte Reviews vol. 1 & 2, Elsevier Applied Science, London, 1987.
2. W. H. Meyer, *Adv. Mater.*, 1998, **10**, 439.
3. Y. J. Wang, J. Qiao, R. Baker and J. Zhang, *Chem. Soc. Rev.*, 2013, **42**, 5768.
4. J. N. de Freitas, A. F. Nogueira and M. A. De Paoli, *J. Mater. Chem.*, 2009, **19**, 5279.

5. F. M. Gray, *Polymer Electrolytes: Fundamental and Technological Applications*, VCH Publishers, New York, 1997.
6. W. Wiczorek, D. Raducha, A. Zalewska and J. R. Stevens, *J. Phys. Chem. B*, 1998, **102**, 8725.
7. A. Karmakar and A. Ghosh, *J. Appl. Phys.*, 2010, **107**, 104113.
8. E. Quartarone and P. Mustarelli, *Chem. Soc. Rev.*, 2011, **40**, 2525.
9. S. Seki, K. Takei, H. Miyashiro and M. Watanabe, *J. Electrochem. Soc.*, 2011, **158**, A769.
10. J. J. Xu, H. Ye and J. Huang, *Electrochem. Commun.*, 2005, **7**, 1309.
11. M. D. Slater, D. Kim, E. Lee, and C. S. Johnson, *Adv. Funct. Mater.*, 2013, **23**, 947.
12. S. Rajendran, M. Sivakumar and R. Subadevi, *Mater. Letts.*, 2004, **58**, 641.
13. G. B. Appetecchi, F. Croce and B. Scrosati, *Electrochim. Acta*, 1995, **40**, 991.
14. F. Croce, G. B. Appetecchi, L. Persi, and B. Scrosati, *Nature*, 1998, **394**, 456.
15. R. Haggemueller, J. E. Fischer and K. I. Winey, *Macromolecules*, 2006, **39**, 2964.
16. J. Zhou and P.S. Fedkiw, *Solid State Ionics*, 2004, **166**, 275.
17. D. K. Pradhan, R. N. P. Choudhary, B. K. Samantaray, N. K. Karan and R. S. Katiyar, *Int. J. Electrochem. Sci.*, 2007, **2**, 861.
18. M. Armand, F. Endres, DR MacFarlane, H. Ohno and B. Scrosati, *Nature Materials*, 2009, 621.
19. Y. S. Ye, J. R. and B. J. Hwang, *J. Mater. Chem. A*, 2013, **1**, 2719.
20. J. Lu, F. Yana and J. Texter, *Prog. Polym. Sci.*, 2009, **34**, 431.
21. H. Ohno, *Electrochemical Aspects of Ionic Liquids*, John Wiley & Sons, Inc., Hoboken, New Jersey. 2005.
22. C. A. Angell, Y. Ansari and Z. Zhao, *Faraday Discuss.*, 2012, **154**, 9.
23. M. P. Singh, R. K. Singh and S. Chandra, *Prog. Mater. Sci.*, 2014, **64**, 73.
24. Shalu, S. K. Chaurasia, R. K. Singh and S. Chandra, *J. Phys. Chem. B*, 2013, **117**, 897-906.
25. I. Tim, J. H. Lee, M. L. Shofner, K. Jacob and R. Tannenbaum, *Polymer*, 2013, **53**, 2402.
26. A. J. Muller, M. L. Arnal, A. L. Spinelli, E. Canizales, C. C. Puig, H. Wang and C. C. Han, *Macromol. Chem. Phys.*, 2003, **204**, 1497.

27. K. L. Singfield, R. A. Chisholm and T. L. King, *J. Chem. Edu.*, 2012, **89**, 159.
28. Shalu, S. K. Chaurasia and R. K. Singh, *RSC Adv.*, 2014, **4**, 50914.
29. K. E. Strawhecker and E. Manias, *Chem. Mater.*, 2003, **15**, 844.
30. A. Keller, G. G. Wood and M. Hikosaka, *Faraday Discuss.*, 1993, **95**, 109.
31. Y. Zhang, H. Huo, J. Li, Y. Shang, Y. Chen, S.S. Funari and S. Jiang, *CrytEngComm*, 2012, **14**, 7972.
32. S. Acierno, N. Grizzuti, H. H. Winter, *Macromolecules*, 2002, **35**, 5043.
33. J. Jin, M. Song and F. Pan, *Thermochim. Acta*, 2007, **456**, 25.
34. V. Sencadas, P. Martins, A. Pitaes, M. Benelmekki, R. L. G. Ribelles and S. Lanceros-Mendez, *Langmuir*, 2011, **27**, 7241.
35. H. Wang, J.K. Keum, A. Hiltner and E. Baer, *Macromolecules*, 2010, **43**, 3359.
36. D. Zhou, X. Mei and J. Ouyang, *J. Phys. Chem. C*, 2011, **115**, 16688.
37. K. Chirssopoulou, K.S. Andrikopoulos, S. Bollas, C. Karageorgaki, D. Chirstofilos, G.A. Voyiatzis and S.H. Anastasiadis, *Macromolecules*, 2011, **44**, 9710.
38. M. J. Avrami, *J. Chem. Phys.*, 1939, **7**, 1103.
39. S. K. Chaurasia, R. K. Singh and S. Chandra, *J. Poly. Sci. Part B: Polym. Phys.*, 2011, **49**, 291.
40. M. P. Scott, C. S. Brazel, M.G. Benton, J. W. Mays, J. D. Holbrey and R. D. Rogers, *Chem. Commun.*, 2002, 1370.
41. N. Winterton, *J. Mater. Chem.*, 2006, **16**, 4281.
42. S. K. Chaurasia, R. K. Singh and S. Chandra, *J. Raman Spectroscopy*, 2011, **42**, 2168.
43. S. K. Chaurasia, R. K. Singh and S. Chandra, *CrytEngComm*, 2013, **15**, 6022.
44. S. K. Chaurasia, R. K. Singh and S. Chandra, *Solid State Ionics*, 2014, **262**, 790.
45. J. B. Zeng, F. Wu, C. L. Huang, Y. S. He and Y. Z. Wang, *ACS Macro Letts.*, 2012, **1**, 965.
46. H. Zhao, Y. Bian, M. Xu, C. Han, Y. Li, Q. Dong and L. Dong, *CrytEngComm*, 2014, **16**, 3896.
47. S. K. Chaurasia, R. K. Singh and S. Chandra, *Solid State Ionics*, 2011, **183**, 32.
48. Shalu, S. K. Chaurasia, R. K. Singh and S. Chandra, *J. Appl. Polym. Sci.*, (2014) Doi: DOI: 10.1002/APP.41456.

49. A. L. Saroj and R. K. Singh, *J. Phys. Chem. Solids*, 2012, **73**, 162.
50. J. Maiz, J. Martin and C. Mijangos, *Langmuir*, 2012, **28**, 12296.
51. J. Li, C. Zhou, G. Wang, Y. Tao, Q. Liu and Y. Li, *Polymer Testing*, 2002, **21**, 583.
52. J. B. Zeng, M. Srivanasan, S. L. Li, R. Narayan and Y. Z. Wang, *Ind. Eng. Chem. Res.*, 2011, **50**, 4471.
53. A. Jeziorny, *Polymer*, 1978, **19**, 1142.
54. T. Ozawa, *Polymer*, 1971, **12**, 150.
55. T. Liu, Z. Mo, S. Wang and H. Zhang, *Polym. Engg. Sci.*, 1997, **37**, 568.
56. L. Wang, G. Li, Y. Chen and S. Li, *Polym. Eng. Sci.*, 2012, **52**, 1621.
57. K. Cao, Q. Wang, Y. C. Zhou, J. M. Sun and Z. Yao, *Ind. Eng. Chem. Res.*, 2012, **51**, 5461.
58. M. L. Di Lorenzo and C. Silvestre, *Prog. Polym. Sci.*, 1999, **24**, 917.
59. A. S. Fischer, M. B. Khalid, M. Widstrom and P. Kofinas, *J. Power Sources*, 2011, **196**, 9767.
60. S. K. Chaurasia and R. K. Singh, *Phase Trans.*, 2010, **83**, 457.
61. T. Wei, S. Pang, N. Xu, L. Pan, Z. Zhang, R. Xu, N. Ma and Q. Lin, *J. Appl. Polym. Sci.*, (2014) Doi: 10.1002/APP.41308.
62. H. E. Kissinger, *Anal. Chem.*, 1957, **29**, 1702.
63. Y. Zheng, M. L. Bruening and G. L. Baker, *J. Polym. Sci. Part B: Polym. Phys.*, 2010, **48**, 1955.
64. A. G. Shtukenberg, Y. O. Punin, E. Gunn, and B. Kahr, *Chem. Rev.*, 2012, **112**, 1805.
65. J. Xi, X. Qiu, S. Zheng and X. Tang, *Polymer*, 2005, **46**, 5702.
66. B. K. Choi, *Solid State Ionics*, 2004, **168**, 123.
67. D. F. Miranda, T. P. Russell and J. J. Watkins, *Macromolecules*, 2010, **43**, 10528.
68. Z. B. Zeng, F. Wu, C. L. Huang, Y. S. He and Y. Z. Wang, *ACS Macro Letts.*, 2012, **1**, 965.

Figure Captions

Figure 1 Heat Flow vs. time plots for (PEO+10 wt.% LiClO₄)+xwt.% BMIMPF₆ for (a) x=0, (b) x=5 and (c) x=10 during isothermal crystallization at different T_c.

Figure 2: The X_t vs. t plot for (PEO+10 wt.% LiClO₄)+xwt.%BMIMPF₆ for (a) x=0 (b) x=5 and (c) x=10 at different T_c's viz. 44, 46, 48, 50 °C.

Figure 3: The rate of crystallization ($G=1/t_{1/2}$) vs. crystallization temperature plots for (PEO+10 wt.% LiClO₄)+x wt.%BMIMPF₆ for (a) x=0 (b) x=5 and (c) x=10 at different crystallization temperatures 44, 46, 48, 50 °C.

Figure 4: Avrami plots using isothermal method for (a) PEO+10 wt.% LiClO₄ (b) (PEO+10 wt.% LiClO₄)+5wt.%BMIMPF₆ and (c) (PEO+10 wt.% LiClO₄)+10wt.%BMIMPF₆ at different crystallization temperatures (viz. T_c = 44, 46, 48, 50 °C).

Figure 5: ln K^{1/n} vs. 1/T_c plot for (PEO+10 wt.% LiClO₄)+10 wt.%BMIMPF₆ during isothermal crystallization.

Figure 6: Heat flow vs. temperature plot for (PEO+10 wt.% LiClO₄)+xwt.%BMIMPF₆ films during non-isothermal crystallization for (a) x=0 (b) x=5 (c) x=10 (d) x=15 and (e) x=20 at different cooling rates by DSC.

Figure 7: X_t vs. temperature plot during non-isothermal crystallization process of (PEO+10 wt.% LiClO₄)+x wt.%BMIMPF₆ for (a) x=0 (b) x=5 (c) x=10 (d) x=15 and (e) x=20 at different cooling rates (viz. 5,10,15,20 °C/min).

Figure 8: X_t vs. time plot during non-isothermal crystallization process of (PEO+10 wt.% LiClO₄)+x wt.%BMIMPF₆ for (a) x=0 (b) x=5 (c) x=10 (d) x=15 and (e) x=20 at different cooling rates (viz. 5,10,15,20 °C/min).

Figure 9: Avrami plots using non-isothermal method of (PEO+10 wt.% LiClO₄)+x wt.%BMIMPF₆ films for (a) x=0 (b) x=5 (c) x=10 (d) x=15 and (e) x=20 at different cooling rates.

Figure 10: Ozawa plots of $\log[-\ln(1-X_T)]$ vs. $\log \phi$ during the non-isothermal crystallization of (PEO+10 wt.% LiClO₄)+x wt.%BMIMPF₆ films for (a) x=0 (b) x=5 (c) x=10 (d) x=15 and (e) x=20.

Figure 11: $\log \phi$ vs. $\log t$ plot of (PEO+10 wt.%LiClO₄)+xwt.%BMIMPF₆ films for (a) x=0 (b) x=5 (c) x=10 (d) x=15 and (e) x=20 at different crystallinity using non-isothermal crystallization method.

Figure 12: Kissinger plot of $\log (\phi/T_p^2)$ vs. $1/T_p$ for (PEO+10 wt.% LiClO₄)+10 wt.% BMIMPF₆.

Figure 13: Image of spherulite growth of (a) PEO+10 wt.% LiClO₄ and (b) (PEO+10 wt.% LiClO₄)+10 wt.% BMIMPF₆ films crystallized at 50 °C at different crystallization time (i) 10 sec, (ii) 30 sec, (iii) 60 sec, (iv) 90 sec and (v) 120 sec.

Figure 14: Spherulites diameter vs. crystallization time plot for (a) PEO+10 wt.% LiClO₄ (b) (PEO+10 wt.% LiClO₄)+10 wt.% BMIMPF₆ films crystallized at 50 °C at different crystallization time.

Table 1: Different crystallization parameters of PEO+10 wt.% LiClO₄+xwt.%BMIMPF₆ films obtained by Avrami plots using isothermal crystallization method.

(PEO+10 wt.% LiClO₄)+x wt.%BMIMPF₆	T_c (°C)	n	K (min⁻ⁿ)	t_{1/2} (min)
(a) x = 0	44	1.48	0.70	0.94
	46	1.40	0.39	1.45
	48	1.65	0.07	3.85
	50	1.86	0.02	3.95
(b) x = 5	44	1.55	0.66	1.02
	46	1.53	0.40	1.35
	48	1.63	0.10	4.09
	50	1.76	0.06	7.09
(c) x = 10	44	1.34	0.33	1.57
	46	1.31	0.11	3.49
	48	1.70	0.02	10.69
	50	1.74	0.01	15.08

Table 2: Different crystallization parameters of (PEO+10 wt.% LiClO₄)+xwt.% BMIMPF₆ films obtained by Avrami plots using non-isothermal crystallization method.

(PEO+10 wt.% LiClO ₄) + x wt.%BMIMPF ₆	Cooling rate ϕ (°C/ min)	n'	Z _t (min ^{-n'})	Z _c	t' _{1/2} (min)
(a) x = 0	5	2.29	0.139	0.674	1.96
	10	2.27	0.516	0.936	1.13
	15	2.01	0.651	0.971	1.02
	20	2.05	0.717	0.986	0.88
(b) x = 5	5	2.539	0.096	0.626	2.16
	10	2.225	0.067	0.961	1.04
	15	2.215	0.839	0.988	1.14
	20	1.742	0.900	0.994	0.85
(c) x = 10	5	2.260	0.138	0.673	1.96
	10	2.242	0.516	0.936	1.13
	15	2.017	0.662	0.972	1.00
	20	1.893	0.751	0.985	0.91
(d) x = 15	5	2.374	0.106	0.638	2.17
	10	2.107	0.311	0.889	1.42
	15	1.387	0.439	0.946	1.07
	20	1.642	0.608	0.975	0.84
(e) x = 20	5	2.199	0.095	0.625	2.47
	10	1.913	0.289	0.883	1.57
	15	1.844	0.398	0.940	1.38
	20	1.503	0.599	0.974	1.13

Table 3: Non-isothermal crystallization parameter of (PEO+10wt.% LiClO₄)+xwt.%BMIMPF₆ at different degrees of crystallinities obtained by Li and Mo method.

(PEO+10 wt.% LiClO ₄)+x wt.%BMIMPF ₆	X_T' in %	F(T)	b
(a) x = 0	10	0.607	1.563
	20	0.840	1.579
	30	0.983	1.662
	40	1.086	1.677
	50	1.171	1.671
	60	1.311	1.784
	70	1.504	1.504
	80	1.727	1.786
(b) x = 5	10	0.629	1.263
	20	0.864	1.180
	30	0.957	1.245
	40	1.059	1.356
	50	1.172	1.172
	60	1.331	1.331
	70	1.570	1.570
	80	1.753	1.583
(c) x = 10	10	0.634	1.485
	20	0.842	1.573
	30	0.973	1.635
	40	1.086	1.695
	50	1.204	1.774
	60	1.343	1.850
	70	1.529	1.529
	80	1.713	1.713
(d) x = 15	10	0.688	1.420
	20	0.932	1.594
	30	1.078	1.714
	40	1.208	1.815
	50	1.334	1.936
	60	1.485	2.060
	70	1.672	2.149
	80	1.820	1.997
(d) x = 20	10	0.714	1.075
	20	0.952	1.267
	30	1.113	1.473
	40	1.254	1.635
	50	1.397	1.818
	60	1.546	1.967
	70	1.722	2.121
	80	1.866	2.126

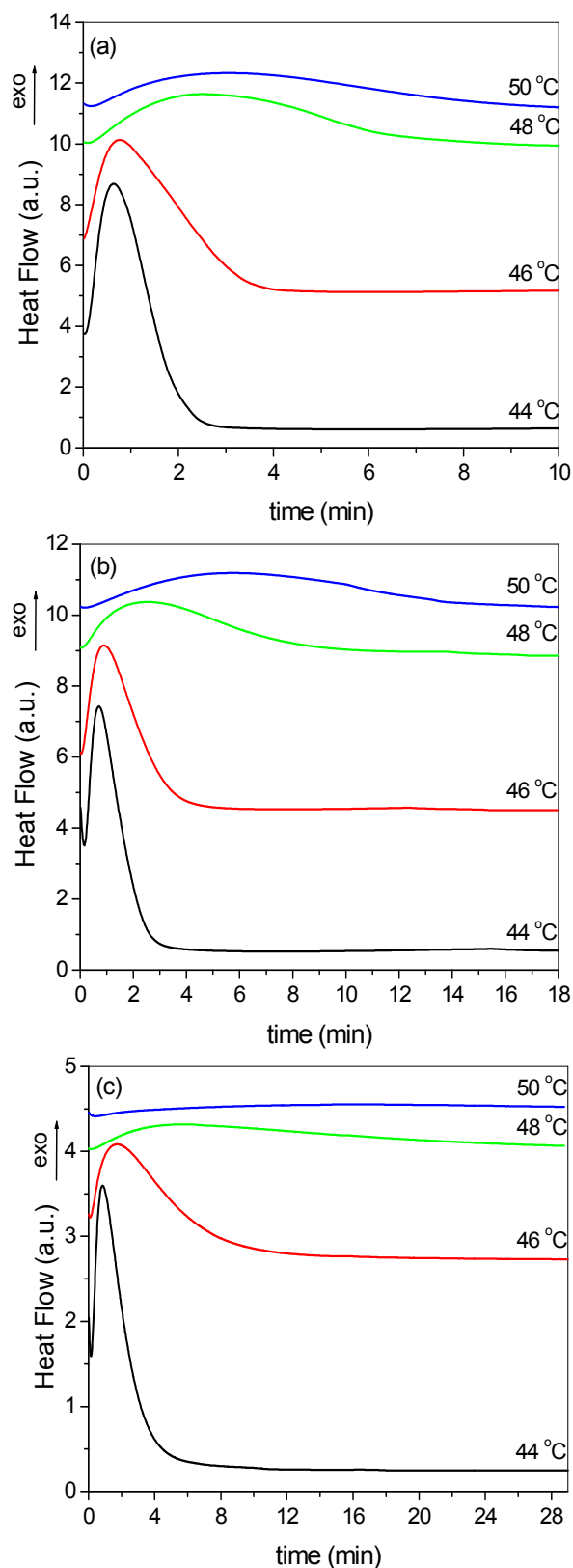


Figure 1 Heat Flow vs. time plots for (PEO+10 wt.% LiClO₄)+xwt.% BMIMPF₆ for (a) x=0, (b) x=5 and (c) x=10 during isothermal crystallization at different T_c .

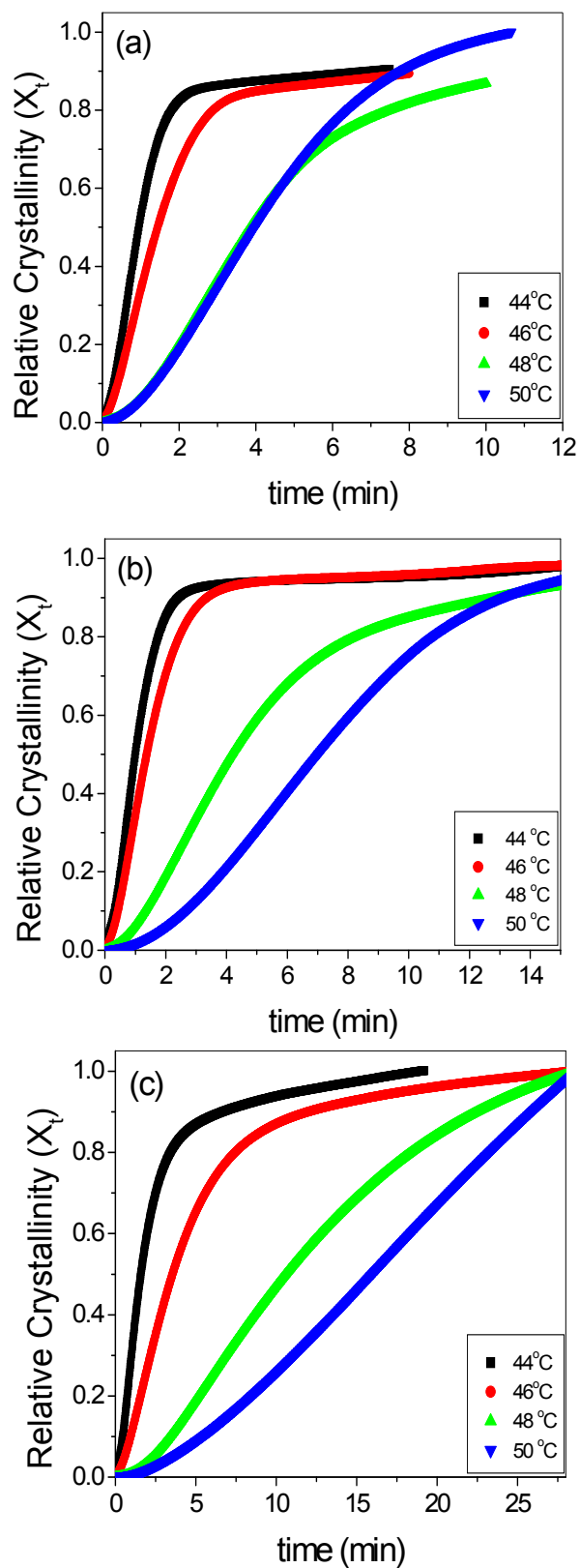


Figure 2: The X_t vs. t plot for (PEO+10 wt.% LiClO₄)+xwt.%BMIMPF₆ for (a) x=0 (b) x=5 and (c) x=10 at different T_c 's viz. 44, 46, 48, 50 °C.

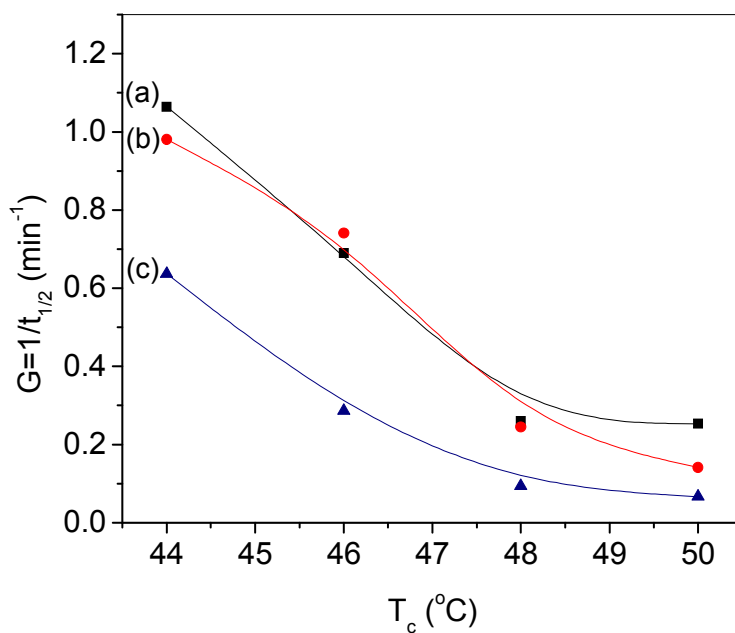


Figure 3: The rate of crystallization ($G=1/t_{1/2}$) vs. crystallization temperature plots for (PEO+10 wt.% LiClO₄)+x wt.%BMIMPF₆ for (a) x=0 (b) x=5 and (c) x=10 at different crystallization temperatures 44, 46, 48, 50 °C.

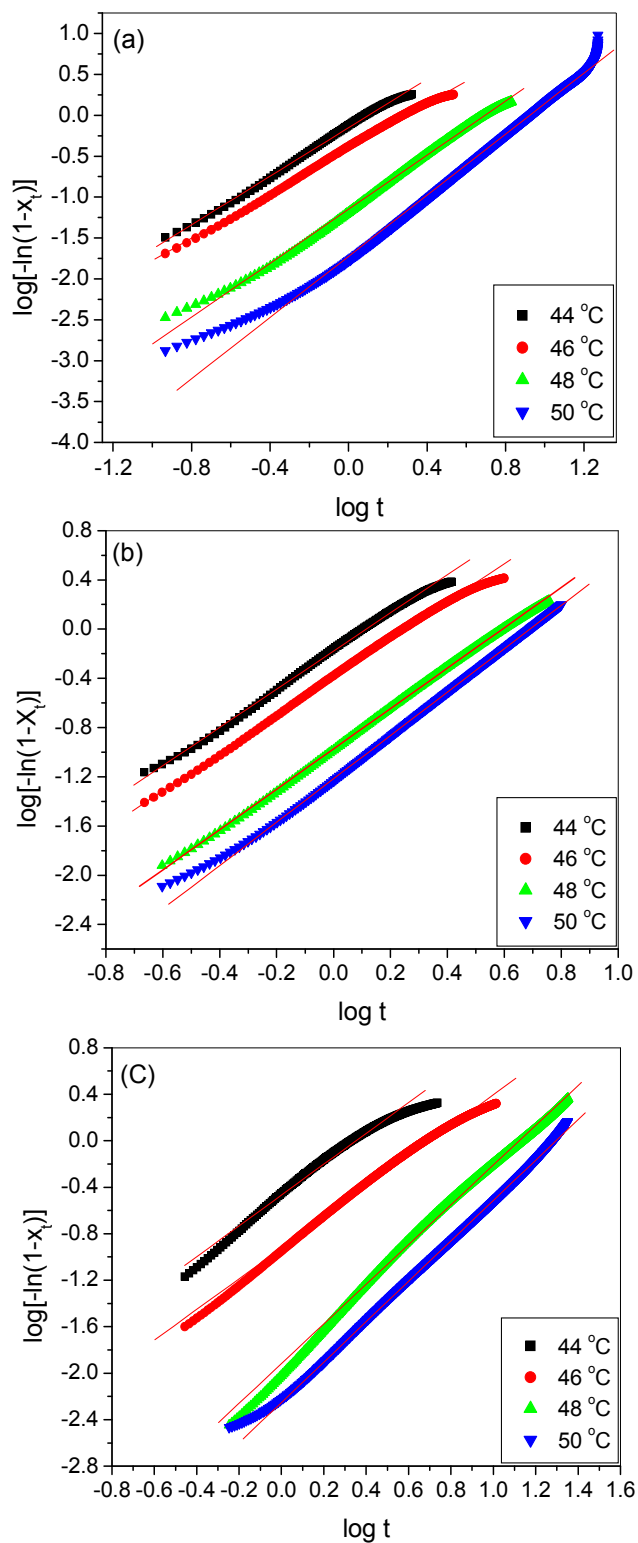


Figure 4: Avrami plots using isothermal method for (a) PEO+10 wt.% LiClO₄ (b) (PEO+10 wt.% LiClO₄)+5wt.%BMIMPF₆ and (c) (PEO+10 wt.% LiClO₄)+10wt.%BMIMPF₆ at different crystallization temperatures (viz. $T_c = 44, 46, 48, 50$ °C).

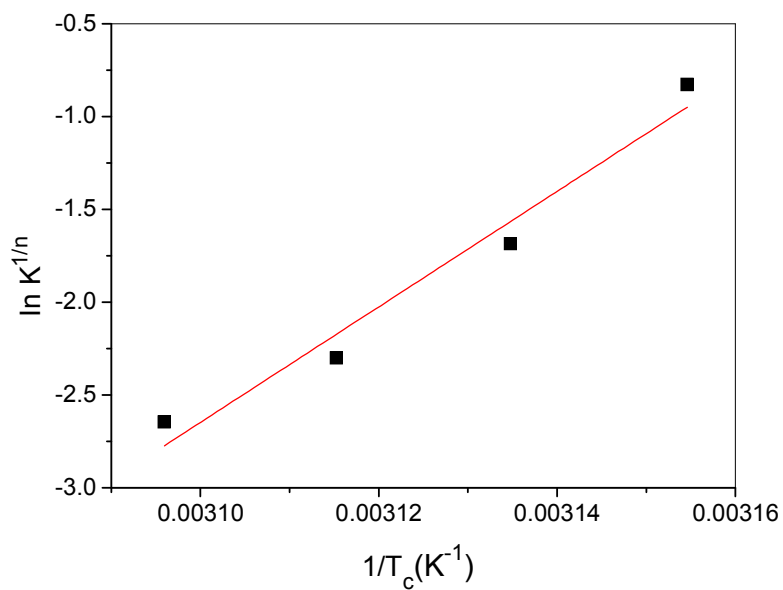


Figure 5: $\ln K^{1/n}$ vs. $1/T_c$ plot for (PEO+10 wt.% LiClO₄)+10 wt.%BMIMPF₆ during isothermal crystallization.

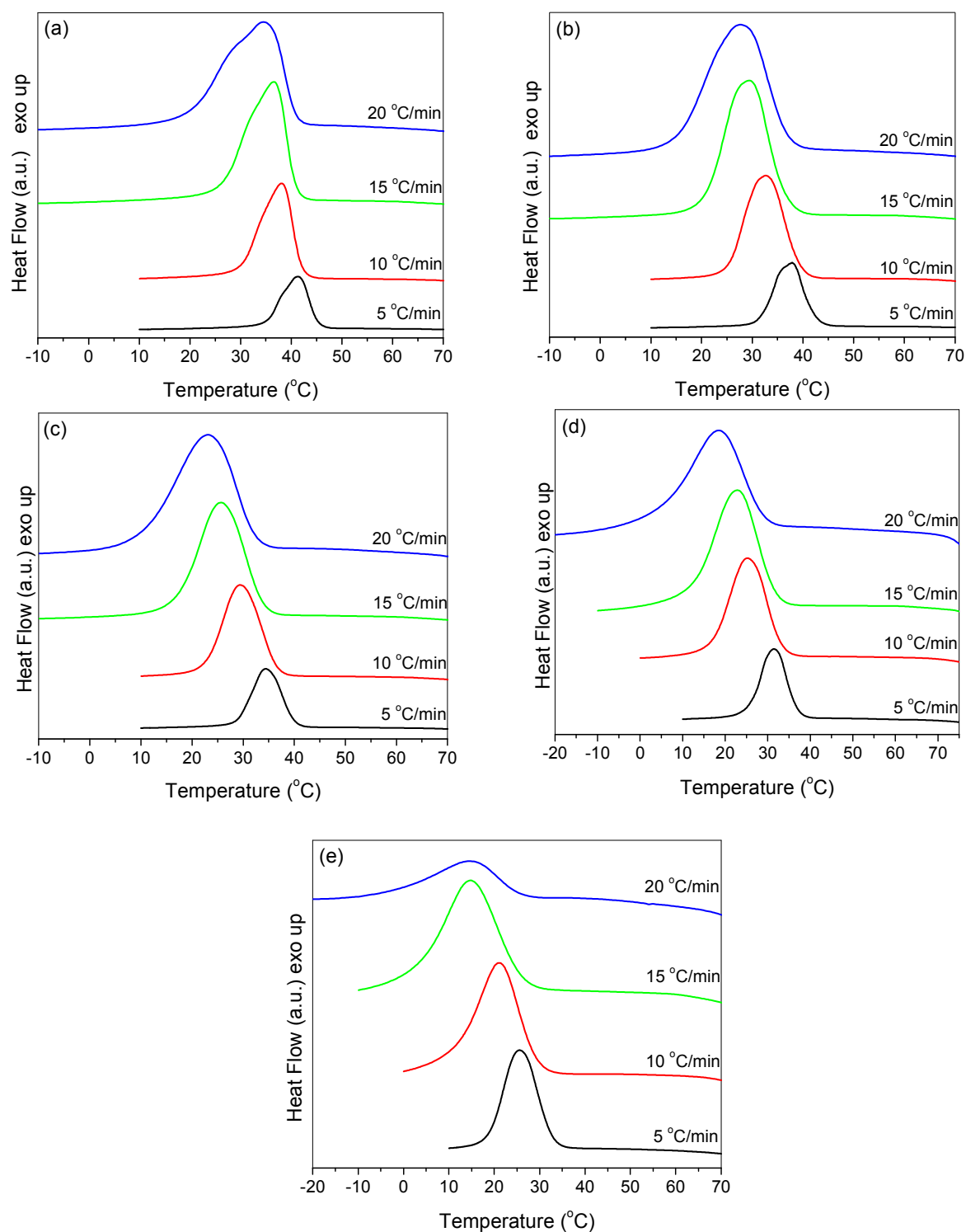


Figure 6: Heat flow vs. temperature plot for (PEO+10 wt.% LiClO₄)+xwt.%BMIMPF₆ films during non-isothermal crystallization for (a) x=0 (b) x=5 (c) x=10 (d) x=15 and (e) x=20 at different cooling rates by DSC.

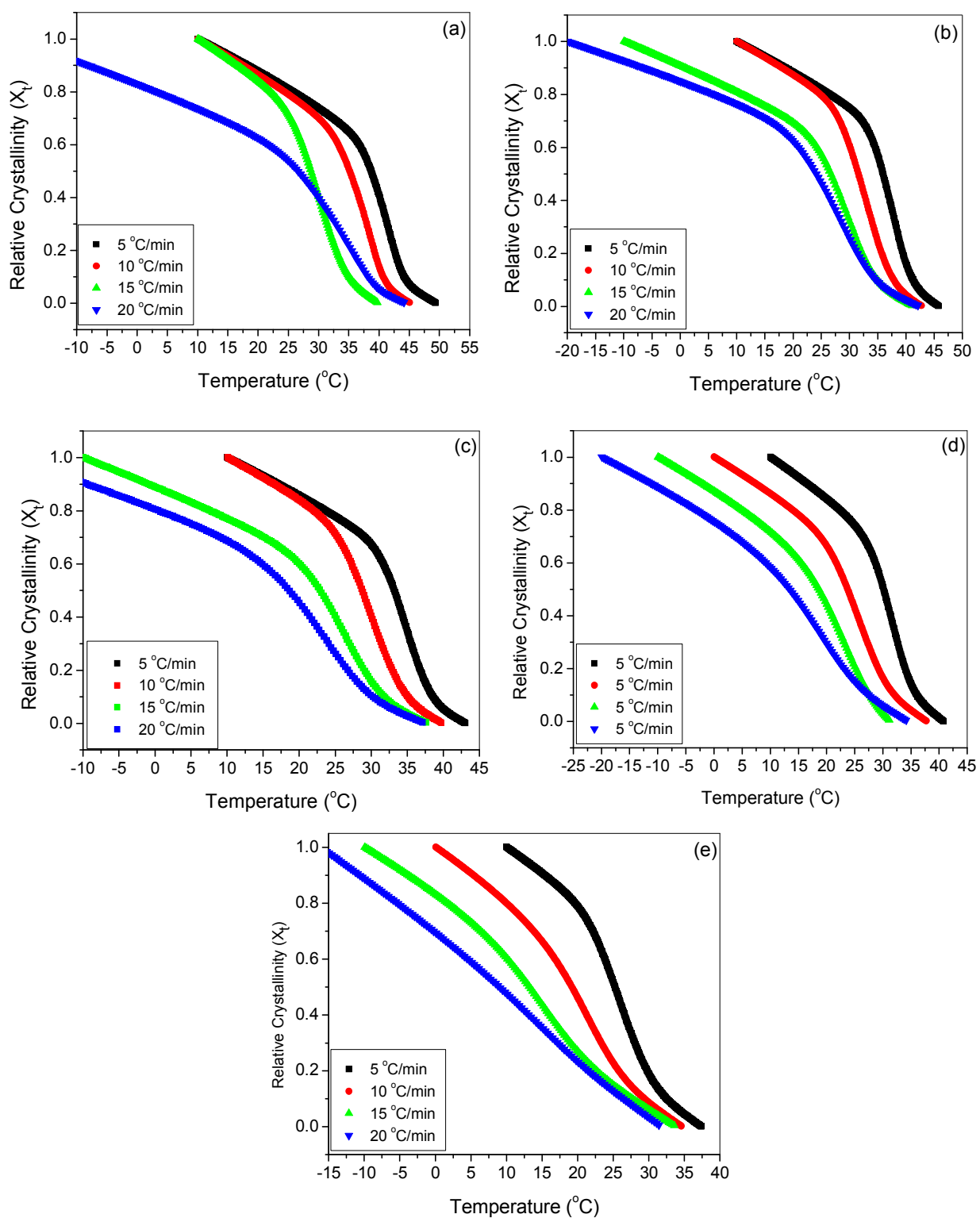


Figure 7: X_t vs. temperature plot during non-isothermal crystallization process of (PEO+10 wt.% LiClO_4)+ x wt.%BMIMPF₆ for (a) $x=0$ (b) $x=5$ (c) $x=10$ (d) $x=15$ and (e) $x=20$ at different cooling rates (viz. 5,10,15,20 $^{\circ}\text{C}/\text{min}$).

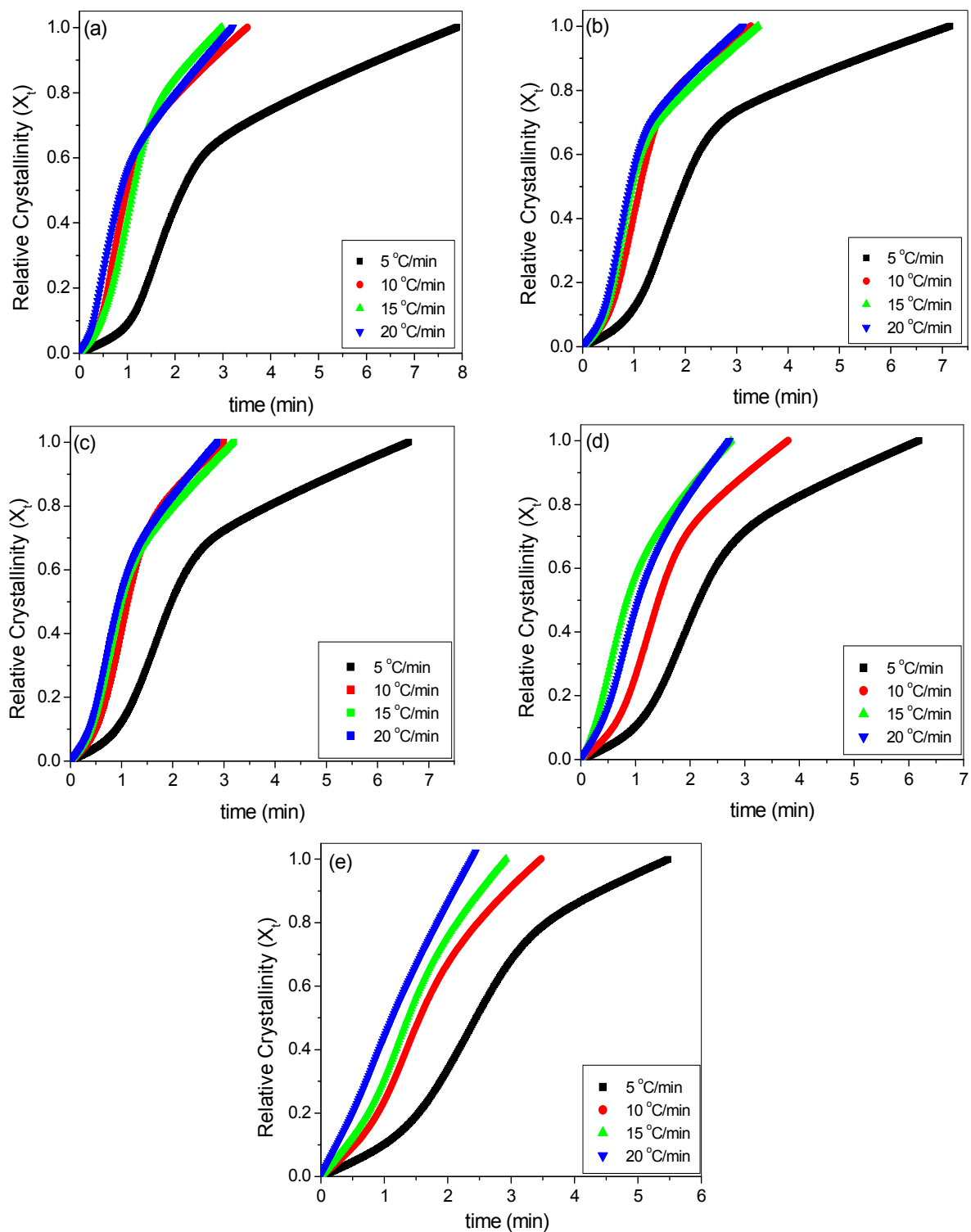


Figure 8: X_t vs. time plot during non-isothermal crystallization process of (PEO+10 wt.% LiClO₄)+x wt.% BMIMPF₆ for (a) x=0 (b) x=5 (c) x=10 (d) x=15 and (e) x=20 at different cooling rates (viz. 5,10,15,20 °C/min).

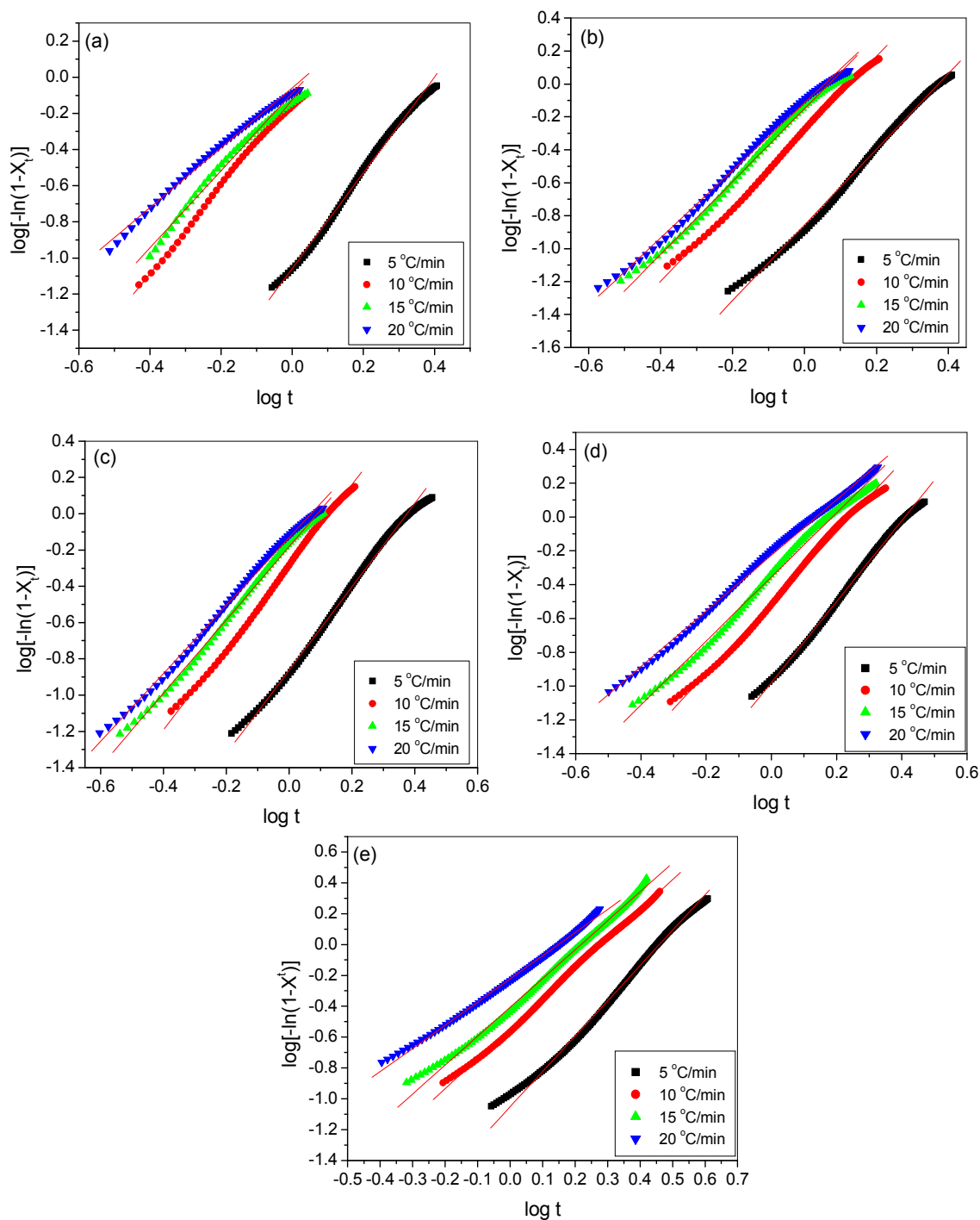


Figure 9: Avrami plots using non-isothermal method of (PEO+10 wt.% LiClO₄)+x wt.%BMIMPF₆ films for (a) x=0 (b) x=5 (c) x=10 (d) x=15 and (e) x=20 at different cooling rates.

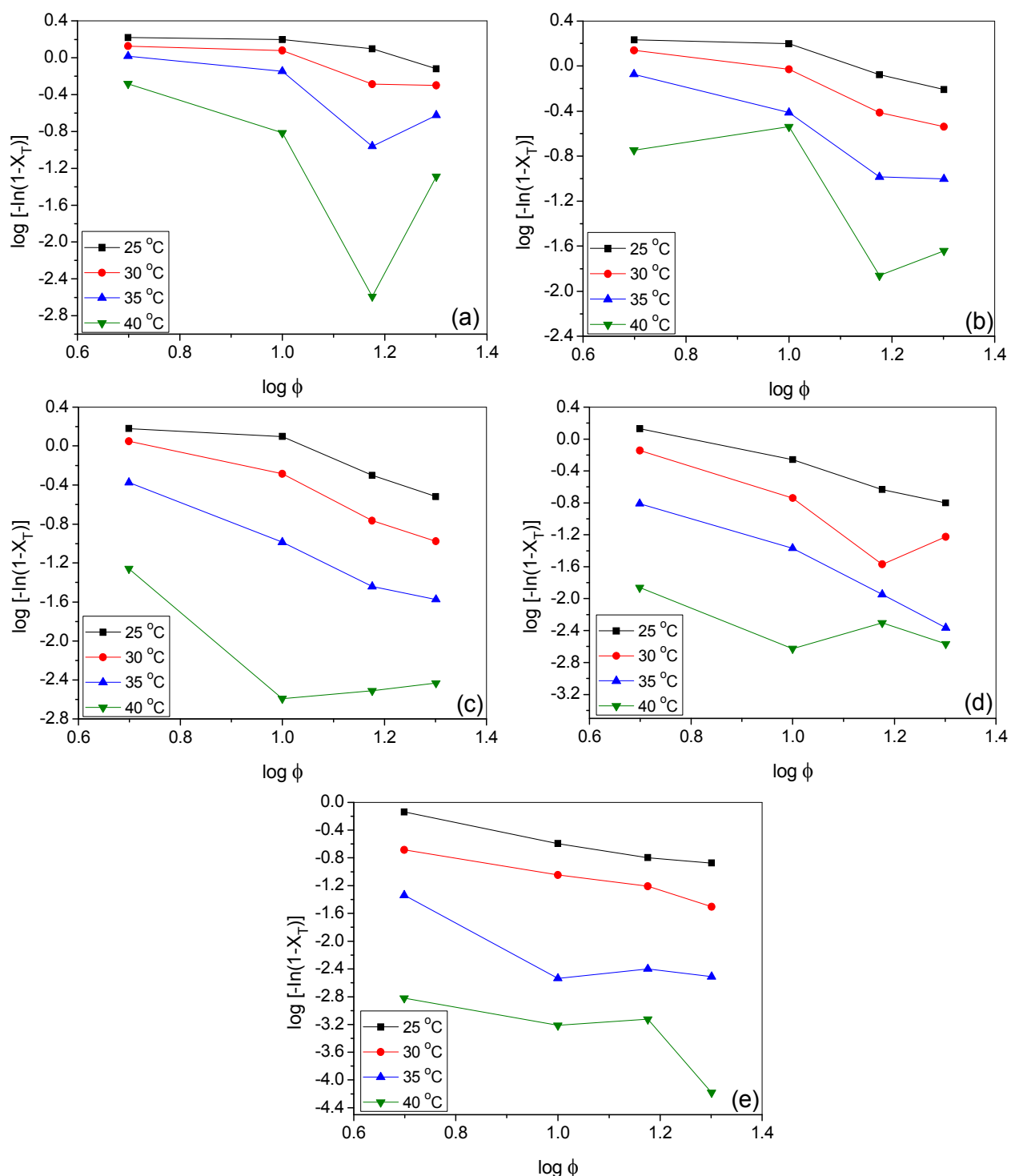


Figure 10: Ozawa plots of $\log[-\ln(1-X_T)]$ vs. $\log \phi$ during the non-isothermal crystallization of (PEO+10 wt.% LiClO₄)+x wt.% BMIMPF₆ films for (a) x=0 (b) x=5 (c) x=10 (d) x=15 and (e) x=20.

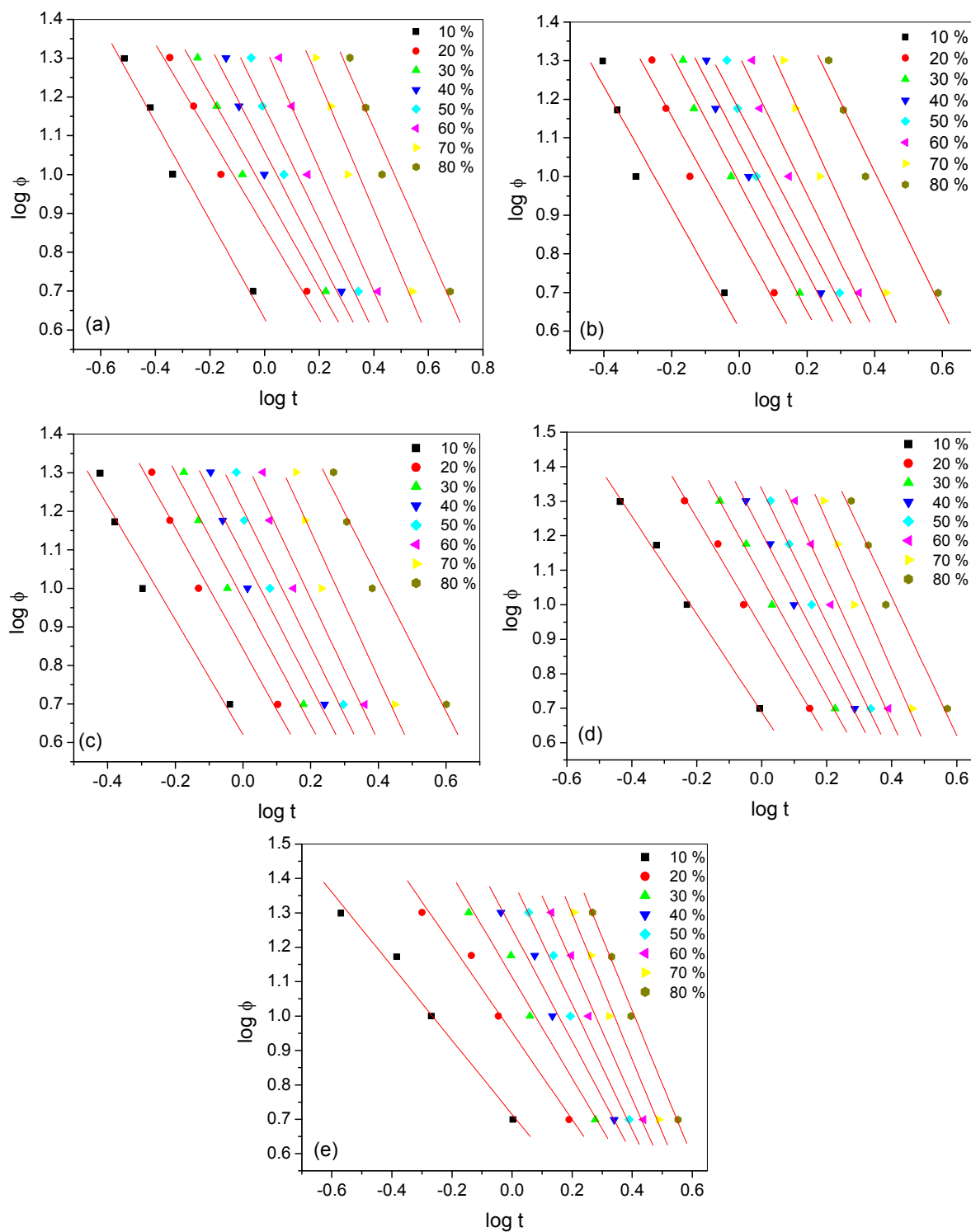


Figure 11: $\log \phi$ vs. $\log t$ plot of (PEO+10 wt.%LiClO₄)+xwt.%BMIMPF₆ films for (a) $x=0$ (b) $x=5$ (c) $x=10$ (d) $x=15$ and (e) $x=20$ at different crystallinity using non-isothermal crystallization method.

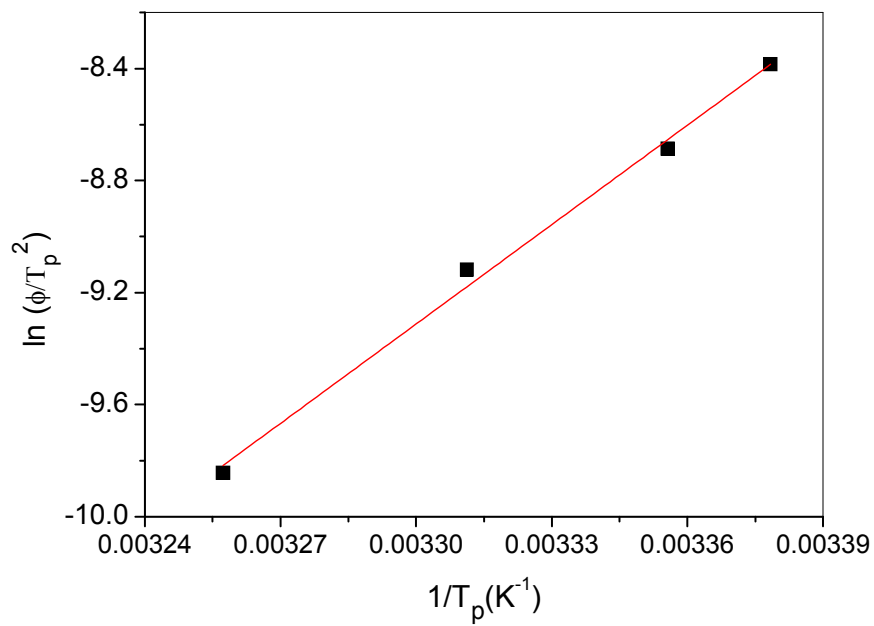


Figure 12: Kissinger plot of $\ln(\phi/T_p^2)$ vs. $1/T_p$ for (PEO+10 wt.% LiClO₄)+10 wt.% BMIMPF₆.

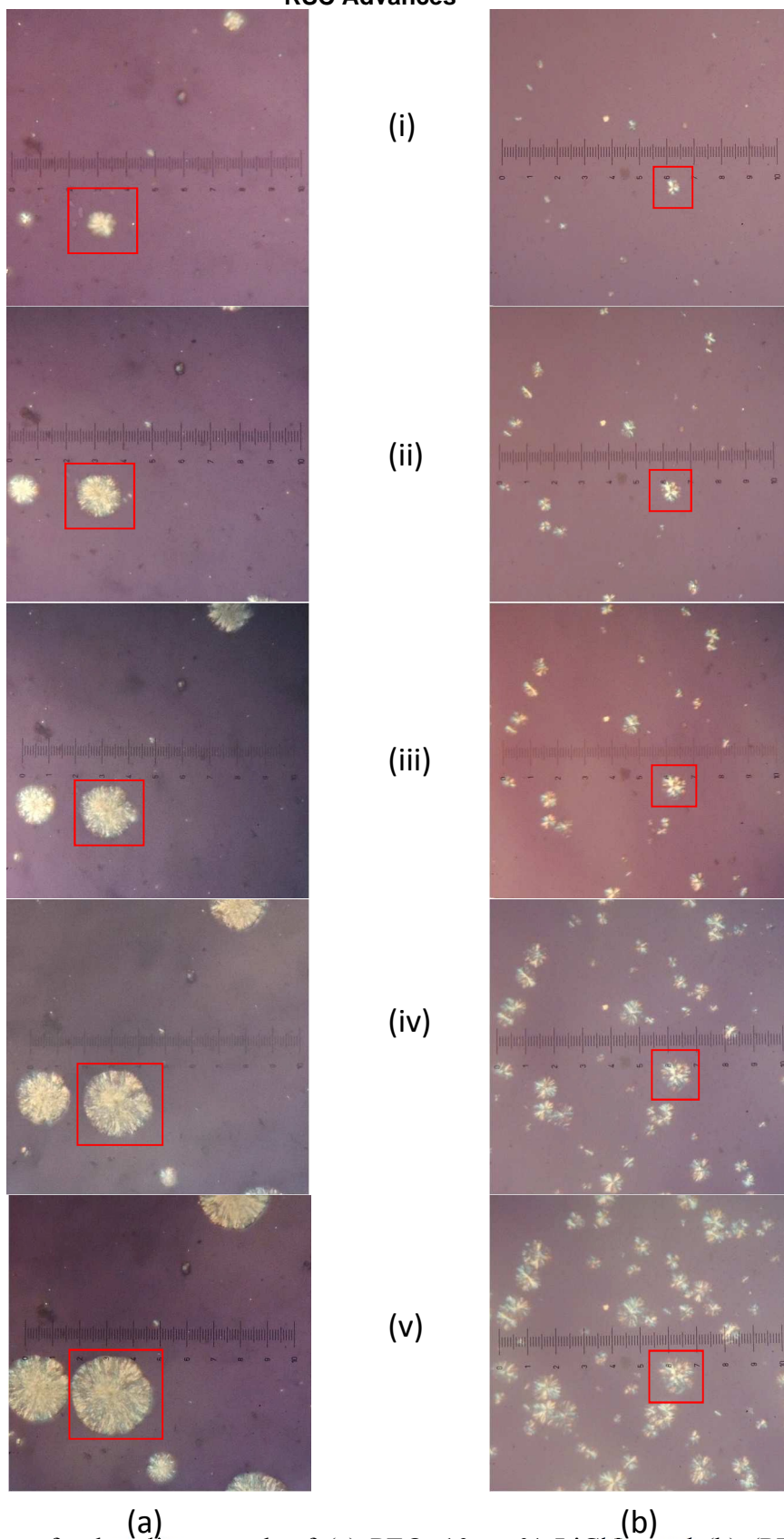


Figure 13: Image of spherulite growth of (a) PEO+10 wt.% LiClO₄ and (b) (PEO+10 wt.% LiClO₄)+10 wt.% BMIMPF₆ films crystallized at 50 °C at different crystallization time (i) 10 sec, (ii) 30 sec, (iii) 60 sec, (iv) 90 sec and (v) 120 sec.

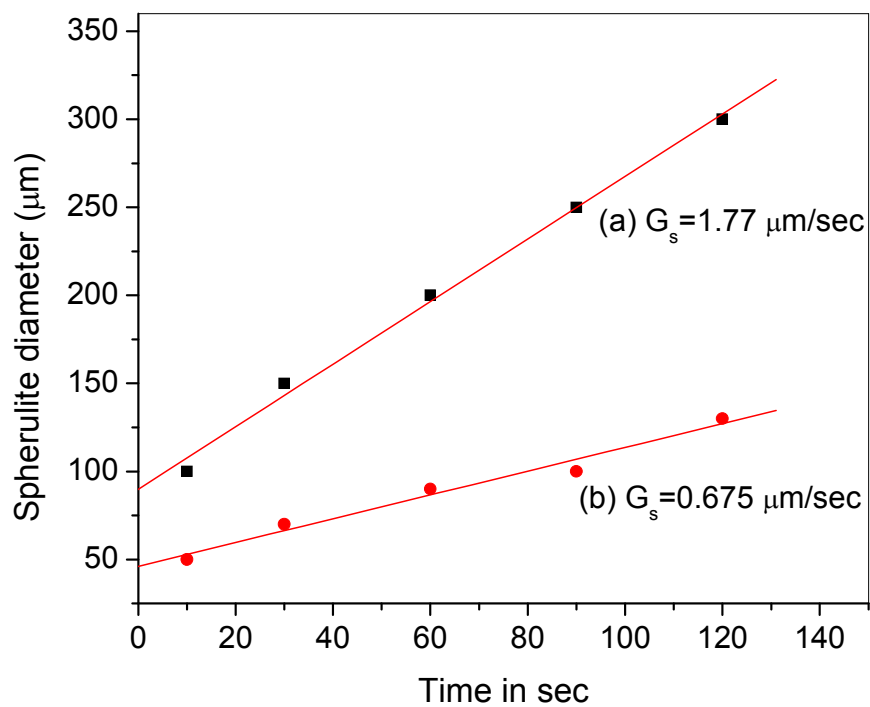


Figure 14: Spherulites diameter vs. crystallization time plot for (a) PEO+10 wt.% LiClO₄ (b) (PEO+10 wt.% LiClO₄)+10 wt.% BMIMPF₆ films crystallized at 50 °C at different crystallization time.